Environmental coupling in ecosystems: From oscillation quenching to rhythmogenesis

Ramesh Arumugam and Partha Sharathi Dutta*
Department of Mathematics, Indian Institute of Technology Ropar, Punjab 140 001, India

Tanmoy Banerjee†
Chaos and Complex Systems Research Laboratory, Department of Physics, University of Burdwan, West Bengal 713 104, India
(Received 11 April 2016; revised manuscript received 27 June 2016; published 10 August 2016)

How landscape fragmentation affects ecosystems diversity and stability is an important and complex question in ecology with no simple answer, as spatially separated habitats where species live are highly dynamic rather than just static. Taking into account the species dispersal among nearby connected habitats (or patches) through a common dynamic environment, we model the consumer-resource interactions with a ring type coupled network. By characterizing the dynamics of consumer-resource interactions in a coupled ecological system with three fundamental mechanisms such as the interaction within the patch, the interaction between the patches, and the interaction through a common dynamic environment, we report the occurrence of various collective behaviors. We show that the interplay between the dynamic environment and the dispersal among connected patches exhibits the mechanism of generation of oscillations, i.e., rhythmogenesis, as well as suppression of oscillations, i.e., amplitude death and oscillation death. Also, the transition from homogeneous steady state to inhomogeneous steady state occurs through a codimension-2 bifurcation. Emphasizing a network of a spatially extended system, the coupled model exposes the collective behavior of a synchrony-stability relationship with various synchronization occurrences such as in-phase and out-of-phase.

DOI: 10.1103/PhysRevE.94.022206

I. INTRODUCTION

For increasing complexity in ecosystems, modeling ecological consequences in continuously changing environmental conditions is one of the central concerns of theoretical ecologists. Various key components like environmental heterogeneity, habitat fragmentation, habitat loss, and seasonal pattern or climatic change profoundly impact many biological phenomena such as the synchrony of oscillating populations, community structure, diversity-stability and synchrony-stability relationship [1–4]. In particular, habitat connectivity through species dispersal among fragmented landscapes play a significant role in determining ecosystem functioning and evolutionary processes [5–7]. Moreover, in spatial ecology, the connectivity of habitats conserves the ecological system by balancing the natural conditions [8]. As population movement prevents local species loss from complete extinction in their local habitat, so it is important to understand the factors which influence the dispersal effect. Numerous coupled nonlinear systems and coupled stochastic oscillators associated with dispersal conceptualize various biological notions starting from oscillations to chaotic behavior [9–11]. Particularly, in the context of species population dynamics, spatially extended dynamical systems with environmental heterogeneity play a leading role in determining the community structure and in maintaining the biodiversity in regional landscapes [2,12,13].

Much less is still known about the effects of species dispersal in dynamic habitats of ecosystems. Recently, in physical generic oscillators, a dynamic environment has been considered in a scheme of indirect coupling to show various synchronization behaviors [14] as well as synchronization of chaotic systems [15], amplitude death, and oscillation death [16–18]. As far as ecological systems are concerned, in general, habitats are highly dynamic rather than static [8,13] where species dispersal takes place in order to maintain the species diversity and persistence [19]. In search of preferential food, sometimes species move a long distance for suitable habitats [20]. While moving from one habitat to another habitat, species get the available food from the environment for their survival. Considering the varying environmental conditions as a dynamic variable, we model the consumer-resource interaction in a dynamic environment along with the presence of dispersion. We consider an ecological oscillator represented by the Rosenzweig-MacArthur model under the simultaneous influence of two different types of couplings: one is the *direct coupling* describing the dispersal of species between spatially separated patches and another one is the *indirect coupling* describing a common dynamic environment for the patches which are connected via dispersal. As far as the ecological environment is concerned, we consider the logistic growth model replicating a dynamic landscape. Our main concern in this paper is to investigate how the interplay of these two separate types of coupling affects the collective dynamics of an ecological system.

In general, the concepts of nonlinear dynamics have been widely used in many studies on complex ecological systems to characterize various natural processes and their ecological perspectives [21,22]. Emphasizing that, in coupled nonlinear systems, *rhythmogenesis* is an interesting dynamical phenomenon, such that the interaction through underlying coupling generates the oscillation from their respective steady states [23–25]. Especially, for regulation and restoration of oscillatory behaviors in various physiological and neuronal systems, rhythmogenesis is utilized as an important consequence of coupled dynamical systems in which the underlying coupling acts as a feedback factor [26–28] and drives the system away from steady state to oscillations. In contrast to the generation of oscillation from steady state, specific

*Corresponding author: parthasharathi@iitrpr.ac.in
†tbanerjee@phys.buruniv.ac.in

 ©2016 American Physical Society

coupling involved in the system can drive coupled oscillators to oscillation quenching states, such as *oscillation death* (OD) and *amplitude death* (AD). In coupled oscillators, OD is created by suppression of oscillations with the formation of stable *inhomogeneous steady states* (IHSS), whereas AD is created by the suppression of oscillations with the formation of stable *homogeneous steady states* [29,30]. As far as ecological models are concerned, oscillation quenching mechanisms emphasize the relationship between dispersal induced stability and dispersal induced synchrony [10,11,31].

In this paper, we show that environmentally coupled ecological systems exhibit both the generation and suppression of oscillations, which are two diametrically opposite phenomena. Using this environmentally coupled model in homogeneous patches (i.e., identical patches), we show amplitude death, oscillation death, formation of inhomogeneous limit cycles, and transition from AD to OD through a codimension-2 bifurcation. In particular, we emphasize that rhythmogenesis can occur along with different synchronized behavior. Although, the uncoupled Rosenzweig-MacArthur (RM) model has simple characteristics, but due to the presence of environmental coupling and dispersal among the fragmented habitats, the system exhibits many interesting dynamics which can be useful in spatial ecology. Moreover, we show that the dynamics of the considered system are also valid for a network of patches which are connected by a common dynamic environment and the system shows rhythmogenesis, perfect synchrony, in-phase synchrony, out-of-phase synchrony, and the formation of a multicluster state.

We organize the paper as follows: First, the environmentally coupled ecological model along with the dynamics of the uncoupled system as well as the dynamics of the environment are described in Sec. II. The linear stability analysis is discussed in Sec. III. Based on this model, the effect of dispersal and it's dynamics are shown in Sec. IV. Further, we extend to a network of ring coupled oscillators, and the robustness of this model is shown in Sec. V. We discuss the results from a dynamical systems point of view and also its ecological interpretation in Sec. VI. Finally, we conclude the results in Sec. VII.

II. MATHEMATICAL MODEL

Taking into account the dispersal between two spatially separated patches in a dynamic environment, we model the consumer-resource interaction in a single system emphasizing the dynamics of the consumer interaction in three ways. First, one is the consumer interaction within the patch, second is the consumer interaction between the connected patches through dispersal, and finally, the consumer interaction through a common dynamic environment. Here, dynamics of the consumer H and the resource V interaction within a patchy habitat is given by the RM model [22,32]. Now, for the interaction between the isolated patches, we consider dispersal of consumer populations between those patches. In fact, immigration and emigration are set by directly coupling the patches with dispersal rate d. Finally, while dispersing between patches, the consumer interacts with the environment and gets the available resource from the environment for their survival. This is potentially important for long distance dispersal of species. To describe the interaction through the environment, we consider another resource E as a common dynamic environment where the uncoupled dynamics of the environment is given by the logistic growth model. Further, the interaction between consumers and environment is governed by a type-II functional response [22,33]. The choice of this particular function is motivated by the fact that it represents a functional response for many consumers. The shape of the function is based on the idea that, at low resource densities, consumers spend most of their time on searching for resources, whereas at high resource densities, they spend most of their time on resource handling [33]. The dynamics of consumer H and resource V for patch 1 and patch 2 along with the common environment E) are modeled as

$$\frac{dV_{1,2}}{dt} = rV_{1,2}\left(1-\frac{V_{1,2}}{K}\right) - \frac{\alpha V_{1,2}}{V_{1,2}+B}H_{1,2}, \tag{1a}$$

$$\frac{dH_{1,2}}{dt} = H_{1,2}\left(\beta\frac{\alpha V_{1,2}}{V_{1,2}+B} - m\right) + d(H_{2,1}-H_{1,2}) + \gamma\frac{\epsilon E}{E+C}H_{1,2}, \tag{1b}$$

$$\frac{dE}{dt} = r_1 E\left(1-\frac{E}{K_1}\right) - \frac{\epsilon E}{E+C}(H_1+H_2), \tag{1c}$$

where subscripts in the variables (V and H) denote the patch index. As we study the dynamics of metapopulation (same species in each patch), parameters are identical for both the patches. Here r is the growth rate of the resource V with K as its carrying capacity, α and B represent the predation rate of the consumer H and half saturation constant, respectively. The predation efficiency and mortality rate of the consumer H are, respectively, given by β and m. In Eq. (1c), the growth rate and the carrying capacity of the environment E are given by r_1 and K_1, respectively. Further, ϵ and γ represent the predation rate and the predation efficiency of the consumer H due to the available resource from the common environment. In the predatory level, C is the half saturation constant of the environment E. The Eqs. (1a)–(1c) emphasize that we use *direct coupling* between the consumers from neighboring patches via the dispersal rate d and *indirect coupling* through the predation rate ϵ of the consumer H.

In all the previous studies [14–18], the environment has been considered as an overdamped oscillator having no intrinsic dynamics other than zero steady state: the environment is modulated in a linear way in the presence of systems that are coupled with it. This is an oversimplified view of any environment and thus, the true essence of a (nonlinear) dynamical environment was missing in those studies. As the environment plays a key role in determining the dynamics of the coupled system, therefore, it is of fundamental interest to study the effect of an environment that is represented with some *realistic* model. Here, not only we take a realistic environment (logistic growth model) but, apart from that, unlike the previous studies [15–18] we also consider the interaction among the environment where the system is to be nonlinear.

Interestingly, it can be shown that the model of the environment considered in [15–18], viz., $\frac{dE}{dt} = -\mathcal{K}E$, where $\mathcal{K}$ is the damping parameter, is a special case of the general model given

in Eq. (1c). When $\epsilon = 0$, from Eq. (1c) the per capita rate of change of the environment is $\frac{1}{E}\frac{dE}{dt} = \frac{f(E)}{E} = r_1(1 - \frac{E}{K_1})$ and hence declines by the quantity $-r_1/K_1$ for each individual added in the population. Let us consider that we perturb E^* by a small quantity s, so the perturbed density is $E^* + s$. Now $\frac{dE}{dt} = \frac{d(E^*+s)}{dt} = \frac{dE^*}{dt} + \frac{ds}{dt} = \frac{ds}{dt} = f(E^* + s)$ as $\frac{dE^*}{dt} = 0$. Expanding the function $f(E^* + s)$ about E^* and neglecting the higher order terms we get $f(E^* + s) = f(E^*) + s\frac{df}{dE}|_{E^*}$. As $f(E^*) = 0$ and $\frac{df}{dE}|_{E^*} = -r_1$, so the approximate form of $\frac{dE}{dt}$ a small distance away from the equilibrium point $E^* = K_1$ is $\frac{ds}{dt} = -r_1 s$, where $r_1 > 0$. Hence, if the steady state of the environment is perturbed by a small amount by some external factors it will actually behave like an overdamped oscillator.

Thus, the environment we have considered here resembles the overdamped model for a smaller perturbation, but additionally, it also accommodates the effect of a larger perturbation exerted by the system. Therefore, the environment considered here, indeed, represents a general model of the environment. In the following, we will emphasize on the results that come due to this nonlinear environment, and which were not observed for the previously considered simplified overdamped model of the environment.

III. STABILITY ANALYSIS

The uncoupled dynamics of the RM model [i.e., Eqs. (1a) and (1b) with $d = 0$ and $\epsilon = 0$] are discussed in [10,32]. Here we briefly discuss it for the sake of clarity. The RM model has two trivial equilibrium points [i.e., $(V^*,H^*) = (0,0)$ and $(V^*,H^*) = (K,0)$] and one nontrivial equilibrium point {i.e., $(V^*,H^*) = (\frac{mB}{\alpha\beta - m}, \frac{Br\beta[K(\alpha\beta - m) - Bm]}{K(\alpha\beta - m)^2})$}. This nontrivial equilibrium point is stable if $\frac{B}{K} > \frac{\alpha\beta - m}{\alpha\beta + m}$ for certain parameter values of K. However, for a range of K values, the nontrivial equilibrium point changes it's stability and rises to a stable limit cycle. Hence, the RM model is in either a steady state or in an oscillation state depending upon different parametric values.

Now, let us investigate the stability of the coupled system given by Eq. (1). The trivial equilibrium points of the environmentally coupled system (1) are given by (0, 0, 0, 0, 0), $(K,0,0,0,0)$, $(0,0,K,0,0)$, $(0,0,0,0,K_1)$, $(K,0,0,0,K_1)$, $(0,0,K,0,K_1)$, $(K,0,K,0,K_1)$, and $(V^o,H^o,V^o,H^o,0)$, and a nontrivial equilibrium point is given by (V^*,H^*,V^*,H^*,E^*). As the expression of the nontrivial equilibrium point is quite cumbersome, here we don't give the expression. However, the expressions for V^o and H^o are given by

$$V^o = \frac{Bm}{\alpha\beta - m}, \text{ and } \quad H^o = -\frac{Br\beta(Bm + Km - K\alpha\beta)}{K(\alpha\beta - m)^2}.$$

The Jacobian matrix $\mathcal{J}$ at the nontrivial equilibrium point (V^*,H^*,V^*,H^*,E^*) is given by

$$\mathcal{J}|_{(V^*,H^*,V^*,H^*,E^*)} = \begin{bmatrix} j_{11} & j_{12} & : & 0 & 0 & : & 0 \\ j_{21} & j_{22} & : & 0 & j_{24} & : & j_{25} \\ \cdots & \cdots & & \cdots & \cdots & & \cdots \\ 0 & 0 & : & j_{11} & j_{12} & : & 0 \\ 0 & j_{24} & : & j_{21} & j_{22} & : & j_{25} \\ \cdots & \cdots & & \cdots & \cdots & & \cdots \\ 0 & j_{52} & : & 0 & j_{52} & : & j_{55} \end{bmatrix},$$

where

$$j_{11} = r - \frac{2rV^*}{K} - \frac{B\alpha H^*}{(B + V^*)^2}, \quad j_{12} = -\frac{\alpha V^*}{(B + V^*)},$$

$$j_{21} = \frac{B\alpha\beta H^*}{(B + V^*)^2}, \quad j_{22} = -d - m + \frac{\alpha\beta V^*}{(B + V^*)} + \frac{\gamma\epsilon E^*}{(C + E^*)},$$

$$j_{24} = d,\ j_{25} = \frac{c\gamma\epsilon H^*}{(C + E^*)^2}, \quad j_{52} = \frac{\epsilon E^*}{(C + E^*)}, \text{ and}$$

$$j_{55} = r_1 - \frac{2r_1 E^*}{K_1} + \frac{2C\epsilon H^*}{C + E^*}.$$

In the Jacobian $\mathcal{J}$, we have block matrices which simplifies the method of finding eigenvalues and the corresponding eigenvalues are given by the expression

$$\lambda_{1,2} = \tfrac{1}{2}(j_{11} + j_{22} - j_{24} \mp \sqrt{4j_{12}j_{21} + (j_{11} - j_{22} + j_{24})^2}),$$

and $\lambda_{3,4,5}$ can be found by the roots of the polynomial $x^3 + ax^2 + bx + c = 0$, where

$$\begin{aligned} a &= -(j_{11} + j_{22} + j_{24} + j_{55}), \\ b &= -j_{12}j_{21} - 2j_{25}j_{52} \\ &\quad + (j_{22} + j_{24})j_{55} + j_{11}(j_{22} + j_{24} + j_{55}), \text{ and} \\ c &= 2j_{11}j_{25}j_{52} + j_{12}j_{21}j_{55} - j_{11}j_{55}(j_{22} + j_{25}). \end{aligned}$$

From these eigenvalues, stability of the equilibrium point for different parameter values can be found. However, it has to be noted that due to the nonlinear nature of the coefficients of the Jacobian, in most of the cases it is very difficult to predict the exact bifurcation points using eigenvalue analysis. Thus, to locate the bifurcation points and curves, we resort to the continuation package XPPAUT [34]. The collective behavior of the coupled systems for different coupling and system parameters are described in the next section.

IV. RESULTS

Emphasizing that, without coupling, the RM model has either a steady state or an oscillatory state depending on the values of parameters, we qualitatively describe the coupled dynamics of system (1) in two distinct conditions: First, we consider the uncoupled patches are in oscillatory state and examine how coupling affects the oscillation suppression states. Whereas, in the second case we consider the uncoupled patches are in an equilibrium condition and investigate how coupling changes this quiescent state in order to establish any possible rhythmogenesis. In the numerical bifurcation analysis [34] we use the fourth-order Runge-Kutta algorithm with step size 0.001.

A. Uncoupled patches are in the oscillatory state

We start with the precondition that in the absence of dispersal (i.e., $d = 0$) between patch 1 and patch 2 and also in the absence of coupling with the environment (i.e., $\epsilon = 0$), the resource V and the consumer H show oscillations. Then, we study the simultaneous effects of dispersal and environmental coupling.

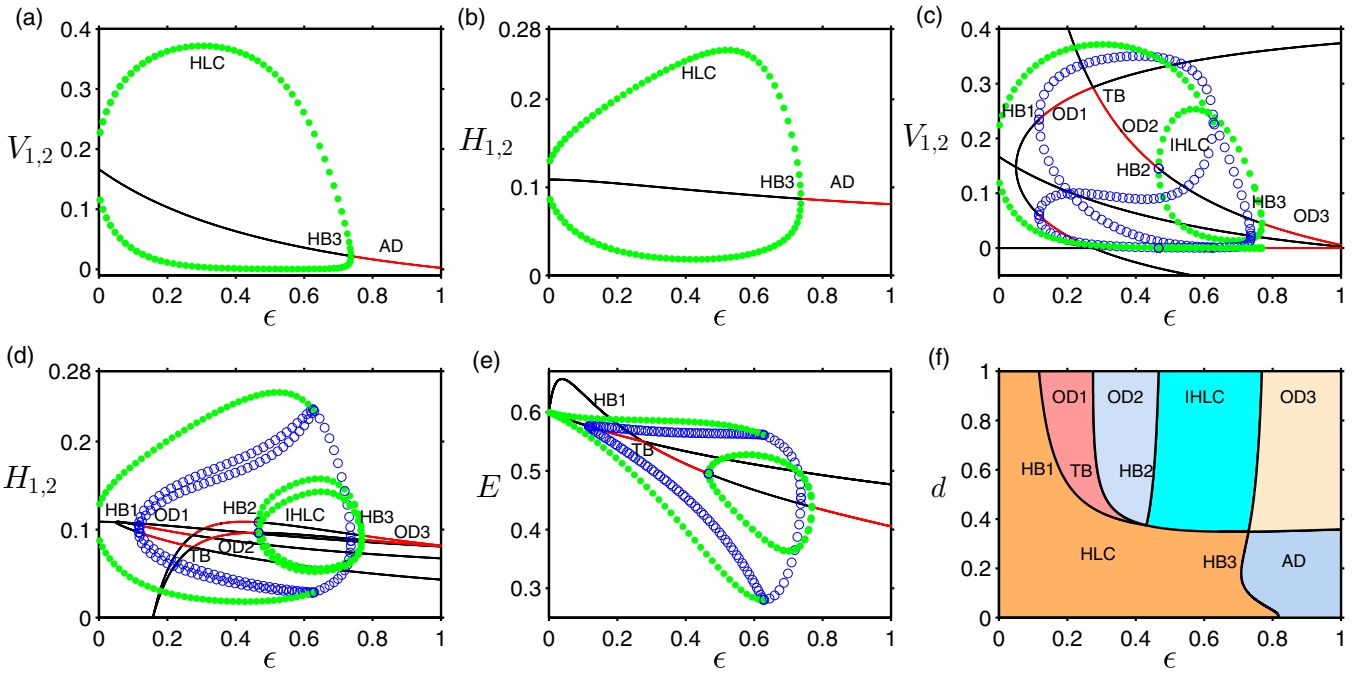

FIG. 1. Oscillation and amplitude death: (a), (b) One parameter bifurcation diagram for varying predation rate ϵ with a lower value of the dispersal rate ($d = 0.2$). (c)–(e) One parameter bifurcation diagram for varying ϵ with a higher dispersal rate ($d = 1$). Red and black curves represent stable and unstable steady states, respectively, whereas green and blue circles represent stable and unstable limit cycles, respectively. Here OD, AD, HB, TB, IHLC, and HLC represent oscillation death, amplitude death, Hopf bifurcation, transcritical bifurcation, inhomogeneous limit cycle, and homogeneous limit cycle, respectively. (f) Two parameter bifurcation diagram in the ϵ-d plane. Other parameters are $r = 0.5$, $K = 0.5$, $\alpha = 1$, $B = 0.16$, $\beta = 0.49$, $m = 0.25$, $\gamma = 0.6$, $r_1 = 0.5$, $K_1 = 0.6$, and $C = 0.6$.

1. Amplitude death in identical oscillators

For a lower dispersion rate (determined by the parameter d), we observe that with increasing predation rate ϵ, AD appears from a stable limit cycle through an inverse supercritical Hopf bifurcation (HB3). Figures 1(a) and 1(b) show the AD state beyond $\epsilon_{HB3} = 0.7367$ for the resource $V_{1,2}$ and the consumer $H_{1,2}$, respectively, for $d = 0.2$. Here in both patch 1 and patch 2, populations are suppressed to homogeneous steady states.

In Ref. [18] it has been shown that an environment modeled by an overdamped oscillator along with the linear modulation from the system can induce AD in the presence of dispersion in generic oscillators. But, the region of AD in the d-ϵ space was shown to be very narrow. In contrast to that, in our present case, once AD occurs at ϵ_{HB3} the system stuck to that state even for higher values of ϵ. This contrast in results may be attributed to the fact that, unlike Ref. [18], here we consider a nonlinear environment and nonlinear coupling. For higher d, symmetry breaking resulted, which is discussed below.

2. Oscillation death for higher dispersal rate d

Beyond a certain dispersal rate d, for increasing predation rate ϵ, an IHSS is created via a pitchfork bifurcation (PB) at $\epsilon_{PB} = 0.05023$: this IHSS gets stable and gives rise to oscillation death (OD1) at $\epsilon_{HB1} = 0.117$. Also, OD2 is created from OD1 through a transcritical bifurcation (TB) at $\epsilon_{TB} = 0.2752$. It is noteworthy that OD1 and OD2 are accompanied by a stable limit cycle, but OD3 that is created through supercritical Hopf bifurcation (HB3) for a higher dispersal value does not share the phase space with any oscillatory state. Moreover, for $m = 0.25$, the dynamics of the environmental resource E is shown in Fig. 1(e). Although, uncoupled dynamic environment E is in steady state, it shows the synchronized oscillating behavior when it's coupled with the oscillating patches.

In Fig. 1(c), OD1 shows inhomogeneous steady states where V_1, V_2, H_1, H_2, and E have nonzero density. But, in the OD2 state, the density of the resource V_i in one patch is almost zero and another is nonzero. Surprisingly, in this situation, the consumers (H_1 and H_2) from both patches have nonzero density both in OD1 and OD2 states. Even though the resource V_i in one patch of OD2 is almost zero, the consumer H_i from that patch survives because of the available resource in the environment. Indeed, in the absence of resource V_i, the survival of consumer H_i is completely supported by the environmental resource E only.

The importance of direct coupling and environmental coupling and it's dynamics are shown for a broader range of parameters using a two parameter bifurcation diagram in ϵ-d space. Figure 1(f) shows the parameter region where the oscillation quenching takes place in directly and indirectly coupled RM model. Each shaded region in Fig. 1(f) determines the dynamics of the coupled system for distinct values of ϵ and d. Moreover, when the dispersal rate d is more than $d_{PB} = 0.3519$ (approximately), OD1, OD2, IHLC, and OD3 occur in the system, whereas only amplitude death occurs for a low dispersal rate.

3. Transition from HLC to IHLC

An interesting finding from Fig. 1(f) is the transition from the homogeneous limit cycle (HLC) to inhomogeneous limit cycles (IHLC) with the variation of the dispersal rate d for

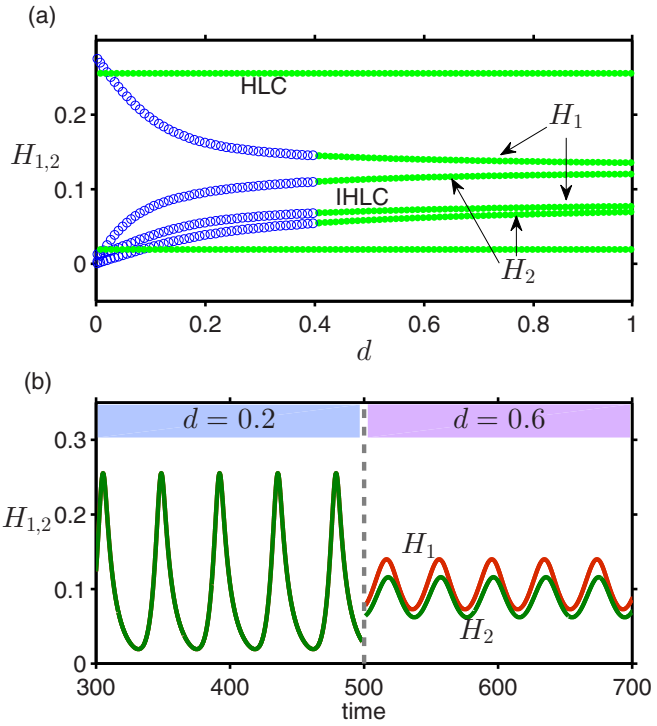

FIG. 2. Transition from HLC to IHLC: (a) One parameter bifurcation diagram of $H_{1,2}$ with varying dispersal rate d. (b) Time series of $H_{1,2}$ which exhibits the direct transition from HLC to IHLC with the change in d. We consider $\epsilon = 0.5$ and all the other parameters are same as in Fig. 1.

a certain range of ϵ. The genesis of this transition can be understood more clearly from the one dimensional bifurcation diagram with d for an exemplary value $\epsilon = 0.5$. From Fig. 2(a) it is seen that for $\epsilon = 0.5$ there exist HLCs even at $d = 0$; additionally they are accompanied by unstable limit cycles [shown in open (blue) circles)]. As d is increased, at d_{HB} the unstable limit cycles get stable to give birth to IHLCs through subcritical Hopf bifurcation, but the original HLCs remain there beyond that point. Thus, beyond d_{HB} we can get a direct transition from the HLC to IHLC for an appropriate choice of initial conditions. Figure 2(b) shows this transition in time series of HLC (at $d = 0.2$) and IHLC ($d = 0.6$) [we take $\epsilon = 0.5$].

In the ϵ space (for a fixed d), it can be seen from Figs. 1(c) and 1(d), that IHLCs are formed at $\epsilon_{HB2} = 0.467$ through a supercritical Hopf bifurcation (HB2) without considering any mismatch in species local dynamics. Further these IHLCs are suppressed to inhomogeneous steady states which give rise to OD3.

4. AD to OD transition

From Fig. 1(f), it is interesting to note that for a higher ϵ value (organized by the HB3 curve) the system shows either AD or OD depending upon the dispersal rate d. Thus, if we fix the value of ϵ in this oscillation suppressed region and vary d, then a continuous direct transition from AD to OD is observed. But, unlike other AD-OD transitions, here the dynamics is governed by the codimension-2 bifurcation.

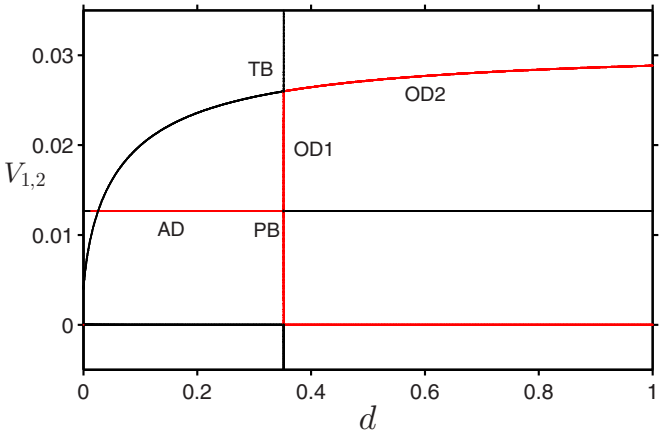

FIG. 3. AD-OD transition: One parameter bifurcation diagram for varying d. Here PB represents pitchfork bifurcation. Red and black curves represent stable and unstable steady states, respectively. Other fixed parameters: $\epsilon = 0.85, \alpha = 1, r = 0.5, K = 0.5, B = 0.16, \beta = 0.49, r_1 = 0.5, K_1 = 0.6, C = 0.6, \gamma = 0.6$, and $m = 0.25$.

This is shown more clearly in Fig. 3, which shows the direct transition from AD to OD with the symmetry breaking of the steady state through pitchfork bifurcation (PB). For a low dispersal rate, system (1) shows AD whereas for increasing dispersal rate, OD1 occurs at $d_{PB} = 0.3519$. Further, with an increase in dispersal d, OD2 is created through TB at $d_{TB} = 0.3519$ which is same as the pitchfork bifurcation point at $d_{PB} = 0.3519$. This shows that $d = 0.3519$ is a point of codimension-2 bifurcation. It is important to note that consumers from patch 1 and patch 2 ($H_{1,2}$) and also the resource $V_{1,2}$ are in nonzero density in the OD1 state whereas the resource $V_{1,2}$ density in OD2 is in a low value.

5. Effect of local dynamics

Relative to the coupling parameters (i.e., d and ϵ), other parameters representing behavioral, morphological, and life history traits (characteristics), such as growth rate r, carrying capacity K, and mortality rate m, also significantly contribute to the dynamics of spatial ecosystems. The resource V from both patch 1 and patch 2 doesn't involve itself in both direct and environmental coupling. However, it indirectly plays the role in determining the oscillation death and amplitude death. Here spatial variation is taken into account, we show the two parameter bifurcation diagram for varying the local parameters (i.e., r, K, and m) along with varying predation rate ϵ.

In Fig. 4, two parameter bifurcation diagrams in the ϵ-r, ϵ-K, and ϵ-m planes are shown with different color shaded regions representing distinct dynamics of the system (1) for different parameters. Figures 1(a)–1(e) depict one particular case of Fig. 4 with a distinct change in each parameter. Here change in growth rate r does not affect much in the OD1 region [shown in Fig. 4(a)] but changes the OD2 region by shrinking inhomogeneous limit cycles. In fact, for higher growth rate r, the inhomogeneous limit cycles vanish and further OD2 and OD3 coincides together and thus forms only one OD. The same conclusion holds for decreasing the carrying capacity K. For a low value of the carrying capacity, no oscillation occurs [shown in Fig. 4(b)]. As far as the local dynamics

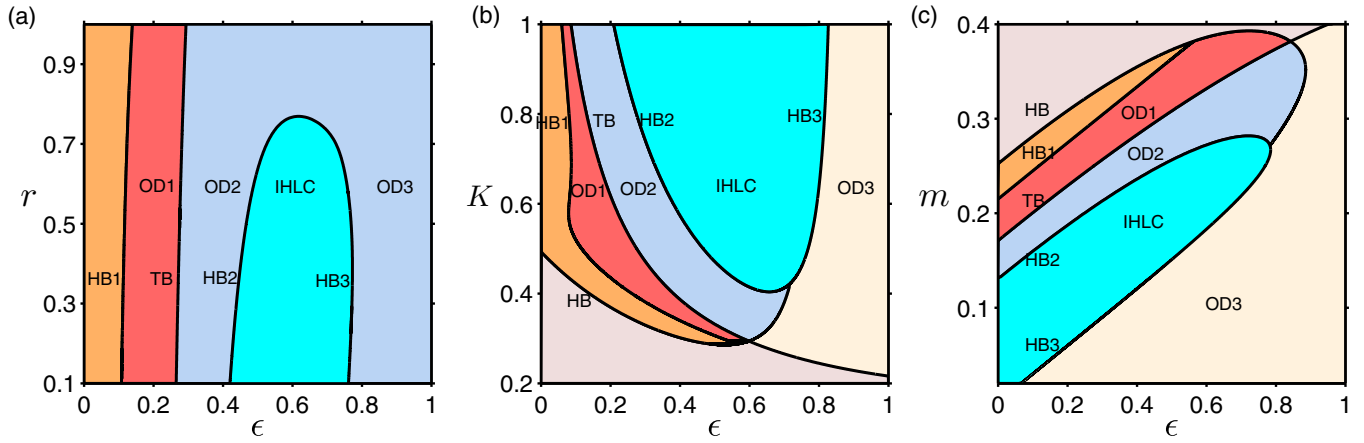

FIG. 4. Local system parameters with environmental coupling parameters: (a) ϵ-r space as a two parameter bifurcation diagram, (b) ϵ-K space, and (c) ϵ-m space. Here fixed parameters are $d = 1$, $\alpha = 1$, $B = 0.16$, $\beta = 0.49$, $r_1 = 0.5$, $K_1 = 0.6$, $C = 0.6$, and $\gamma = 0.6$. In each diagram, other fixed parameters are $r = 0.5$, $K = 0.5$, and $m = 0.25$.

of the patch is concerned, mortality rate m is an important factor in heterogeneous fragmented landscapes. We check the dynamics for a varying mortality rate and predation rate. For an increasing mortality state, the OD region and inhomogeneous limit cycles disappear [shown in Fig. 4(c)]. At a low mortality rate, IHLC and OD occur whereas for higher mortality rate, we have only homogeneous limit cycles along with oscillation death through HB3. Importantly, both environmental coupling parameters and local dynamical parameters determine the dynamics of the considered system.

B. Uncoupled patches are in the equilibrium state

All the results shown in the previous section are based on the initial assumption that the dynamics of an uncoupled system is in an oscillatory state. Now we explore the effect of direct and indirect coupling when the uncoupled patches are in an equilibrium state. We set the individual uncoupled patches to be in a steady state by choosing the proper value of the mortality rate m of the consumer H.

1. Rhythmogenesis and oscillation death

In this section, we set each patch in an equilibrium state by choosing the mortality rate of the consumer as $m = 0.3$. We check the dynamics of the system (1) in two different cases. One is the absence of direct coupling and another is considered with direct coupling along with coupling through the environment.

Case I. Absence of direct coupling. In the absence of direct coupling (i.e., $d = 0$), we show the dynamics of system (1) using a one parameter bifurcation diagram for varying ϵ with resource density in Fig. 5(a). Interestingly, oscillations are created at $\epsilon_{HB} = 0.1605$ in the presence of environmental coupling alone through supercritical Hopf bifurcation. The generation of oscillation through coupling is termed as rhythmogenesis in the literature [23,24]. Hence, the presence of environmental coupling drives the steady state to an oscillatory state and creates rhythmogenesis with a finite period of oscillation. Moreover, torus bifurcation is created here with chaotic dynamics [shown in Fig. 5(a)]. The torus bifurcation is associated with the Neimark-Sacker bifurcation of the Poincaré map of a limit cycle in an ordinary differential equation. Sometimes torus bifurcation is also referred as secondary Hopf bifurcation and occurs at the double-Hopf bifurcation of the equilibrium point in a continuous dynamical system. In Fig. 5(a), torus bifurcation occurs at $\epsilon_{TR} = 0.652$ with a pair of eigenvalues $0.6907 \pm 0.7232i$ which has unit modulus. We check back and forth of this torus bifurcation for different ϵ values. When $\epsilon = 0.6518$, a pair of Floquet multipliers $0.6905 \pm 0.7224i$ exists with absolute value 0.9993 whereas when $\epsilon = 0.6528$, a pair of Floquet multipliers $0.6917 \pm 0.7267i$ exists with absolute value 1.003. Further, corresponding trajectories and a phase space of chaotic dynamics are shown in Figs. 5(d) and 5(e).

As there is no dispersal (i.e., no direct coupling) between the patches, only environmental coupling plays a role in determining the dynamics here. In Fig. 5(a), it is shown that two limit cycles occur together with a torus bifurcation. The upper one is in out-of-phase synchrony, whereas the lower one shows the perfect synchrony between the patches. In fact, in the lower one, torus bifurcation occurs. From this two limit cycles, depending on the initial conditions, we get either perfect synchrony or out-of-phase synchrony. Figures 5(b) and 5(c) show time series of perfect and out-of-phase synchrony, respectively, of the resource $V_{1,2}$ for fixed $\epsilon = 0.5$, but with different initial conditions. For increasing predation rate ϵ, the system shows the chaotic behavior and perfect synchrony. At $\epsilon = 0.76$, in Figs. 5(d) and 5(e) time series and phase space are shown, respectively. Hence, perfect synchrony, out-of-phase synchrony, and chaotic dynamics occur with the presence of indirect coupling.

Case II. Presence of direct and indirect coupling. With the presence of direct coupling (i.e., $d \neq 0$), the occurrence of oscillation death is shown in Fig. 5(f) for increase in predation rate ϵ. For this case also, rhythmogenesis occurs through the variations in the coupling parameter ϵ. In fact, coupling drives the steady state to an oscillatory state which further quenched to oscillation death as mentioned in the earlier section. First oscillations are generated through supercritical Hopf bifurcation at $\epsilon_{HB} = 0.1301$ and then OD1 is created at $\epsilon_{HB1} = 0.2438$ by symmetry breaking of the steady state

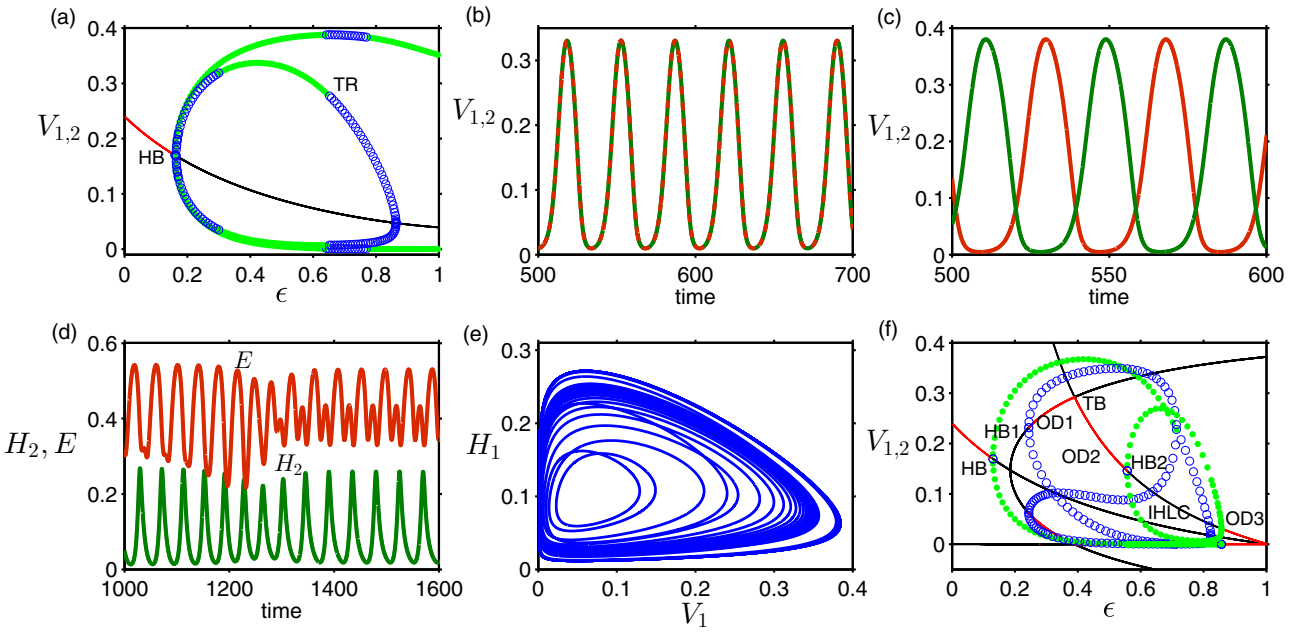

FIG. 5. (a) One parameter bifurcation diagram for varying ϵ with $d = 0$. TR represents torus bifurcation. Other fixed parameters are $\alpha = 1, r = 0.5, K = 0.5, B = 0.16, \beta = 0.5, r_1 = 0.5, K_1 = 0.6, C = 0.5, \gamma = 0.5$, and $m = 0.3$. (b) Perfect synchrony for $\epsilon = 0.5$ with the initial condition $(V_1, H_1, V_2, H_2, E) = (0.28, 0.051, 0.24, 0.052, 0.55)$. (c) Out-of-phase synchrony for $\epsilon = 0.5$ with a different initial condition $(V_1, H_1, V_2, H_2, E) = (0.297, 0.145, 0.016, 0.0308, 0.5)$. (d) Time series of chaotic behavior for $\epsilon = 0.76$ (after the TR). (e) Phase space of the chaotic time series. In (b)–(e), the parameters are the same as in (a). (f) One parameter bifurcation diagram for varying ϵ with fixed $d = 1$. Here other parameters are $\alpha = 1, r = 0.5, K = 0.5, B = 0.16, \beta = 0.5, r_1 = 0.5, K_1 = 1, C = 0.5, \gamma = 0.5$, and $m = 0.3$.

through pitchfork bifurcation. Further, OD2 is created through transcritical bifurcation at $\epsilon_{TB} = 0.3899$. Moreover, inhomogeneous limit cycles arise at $\epsilon_{HB2} = 0.557$ which are further suppressed to OD3 at $\epsilon = 0.857$ [shown in Fig. 5(f)].

For the fixed direct coupling parameter d, we have shown the various dynamics of system (1) with variations in environmental coupling parameters. In contrast, for the fixed environmental coupling parameter, we find the dynamics for varying the direct coupling parameter. We show the one parameter bifurcation diagram for varying the coupling strength d in Fig. 6(a). It is important to note that here we always start with a steady state in uncoupled patches. OD is created at $d_{OD} = 0.8698$ by symmetry breaking of the steady state through PB.

2. *Perfect and out-of-phase synchrony*

As we use environmental coupling to connect the indirect interaction of the consumers between the patches via a common environment, parameters such as predation rate ϵ and predation efficiency γ in the environmental coupling determine the intrinsic dynamics of the system. So far, for changing predation rate ϵ, we determine the dynamics of

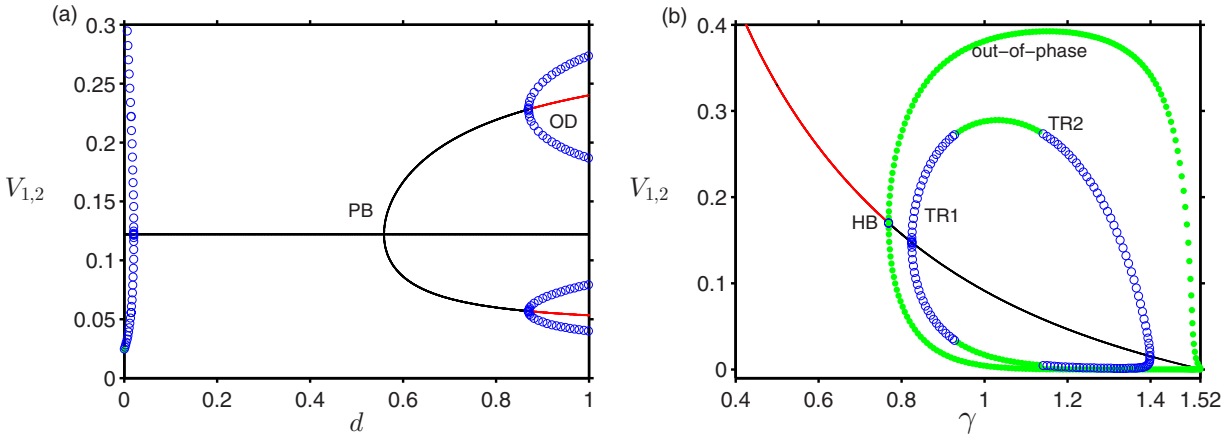

FIG. 6. Direct coupling: (a) One parameter bifurcation diagram for varying d with the fixed parameters $\epsilon = 0.1636, \alpha = 1, r = 0.5, K = 0.5, B = 0.16, \beta = 0.5, r_1 = 0.5, K_1 = 0.6, C = 0.5, \gamma = 0.5$, and $m = 0.27$. (b) One parameter bifurcation diagram for varying predation efficiency γ for fixed parameters $d = 0, \alpha = 0.6, r = 0.5, K = 0.5, B = 0.16, \beta = 0.5, r_1 = 0.5, K_1 = 0.7, C = 0.3, \epsilon = 0.3$, and $m = 0.3$.

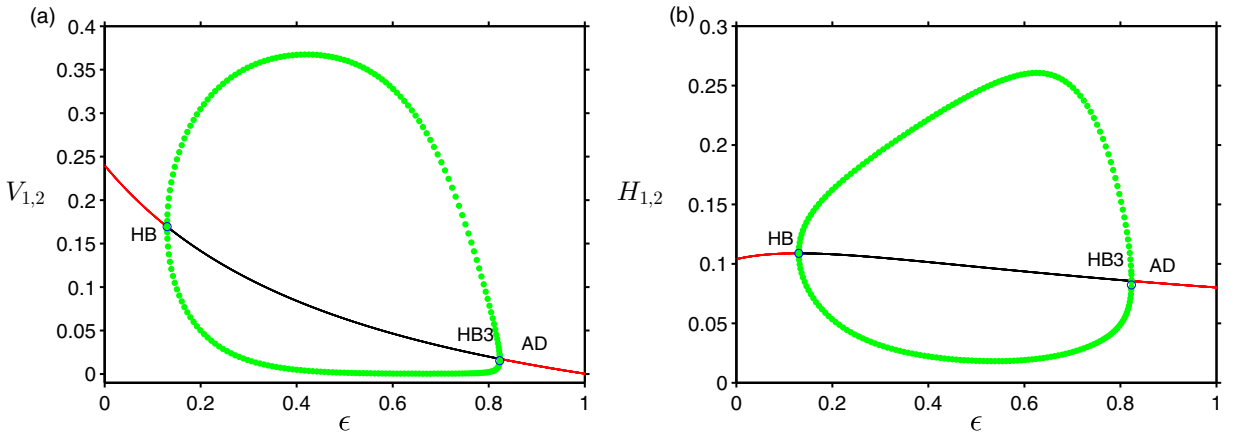

FIG. 7. Amplitude Death: (a), (b) One parameter bifurcation diagrams for varying ϵ for the fixed parameters $\alpha = 1$, $r = 0.5$, $K = 0.5$, $B = 0.16$, $\beta = 0.5$, $r_1 = 0.5$, $K_1 = 1$, $C = 0.5$, and $m = 0.3$. Other fixed parameters are $\gamma = 0.5$ and a low value in direct coupling strength $d = 0.3$.

this system. However, for increasing predation efficiency γ, we show other interesting dynamics using the one parameter bifurcation diagram in Fig. 6(b). As mentioned earlier in Fig. 5, here oscillations are created through coupling and further we have out-of-phase synchrony, in-phase synchrony, and perfect synchrony among the patches. Also, we have torus bifurcation where the stable limit cycles transitioned to unstable limit cycles. For a particular γ value, we have perfect and out-of-phase synchrony which occur completely depending on the initial conditions.

3. *Rhythmogenesis and AD*

As we start with a fixed steady state in the uncoupled patch, in all the cases for an increase in predation rate, oscillations are created and further suppressed to inhomogeneous steady states. In another parametric setup and for a low value of direct coupling strength d, we have rhythmogenesis (homogeneous limit cycles) at $\epsilon_{HB} = 0.1301$ and suppressed steady states at $\epsilon = 0.823$ occur for increasing predation rate ϵ. In this case, one parameter bifurcation diagrams for both resource and consumer are given in Figs. 7(a) and 7(b), respectively.

The robustness of the creation of oscillation and oscillation death is identified by ϵ-d space and ϵ-γ space in Figs. 8(a) and 8(b), respectively, using two parameter bifurcation diagrams. For low to high dispersal rate d, rhythmogenesis always occurs at $\epsilon_{HB} = 0.1301$ which is a limit point to oscillation creation. For a low dispersal rate, rhythmogenesis and AD take place whereas for higher dispersal rate, both rhythmogenesis, oscillation death, and IHLC occur [shown in Fig. 8(a)]. Also, for increasing predation efficiency in the environmental coupling, we have a death state and inhomogeneous limit cycles. However, for a higher predation rate and predation efficiency, only oscillation death (OD3) occurs [shown in Fig. 8(b)].

V. NETWORK STRUCTURE

We extend the system (1) to a network consisting N number of patches coupled by a common dynamic environment E and also dispersal takes place among the connected patches. Using a ring type coupled network (i.e., we consider the periodic boundary condition), we set that each patch is connected to its nearest neighbor. So the dynamics of the consumer H and

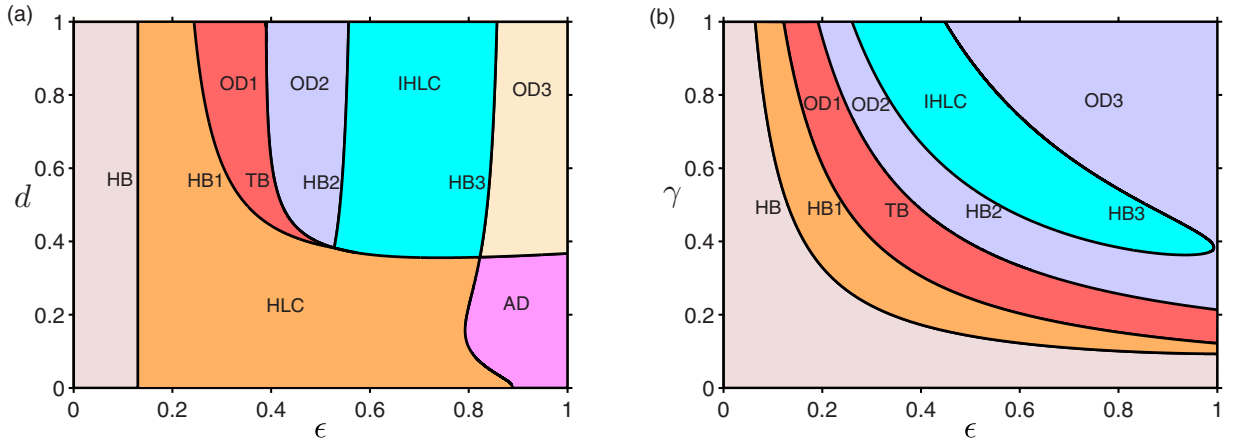

FIG. 8. Two parameter bifurcation diagrams: (a) ϵ-d space for fixed $\gamma = 0.5$, and (b) ϵ-γ space for fixed $d = 1$. Other fixed parameters are $\alpha = 1$, $r = 0.5$, $K = 0.5$, $B = 0.16$, $\beta = 0.5$, $r_1 = 0.5$, $K_1 = 1$, $C = 0.5$, and $m = 0.3$.

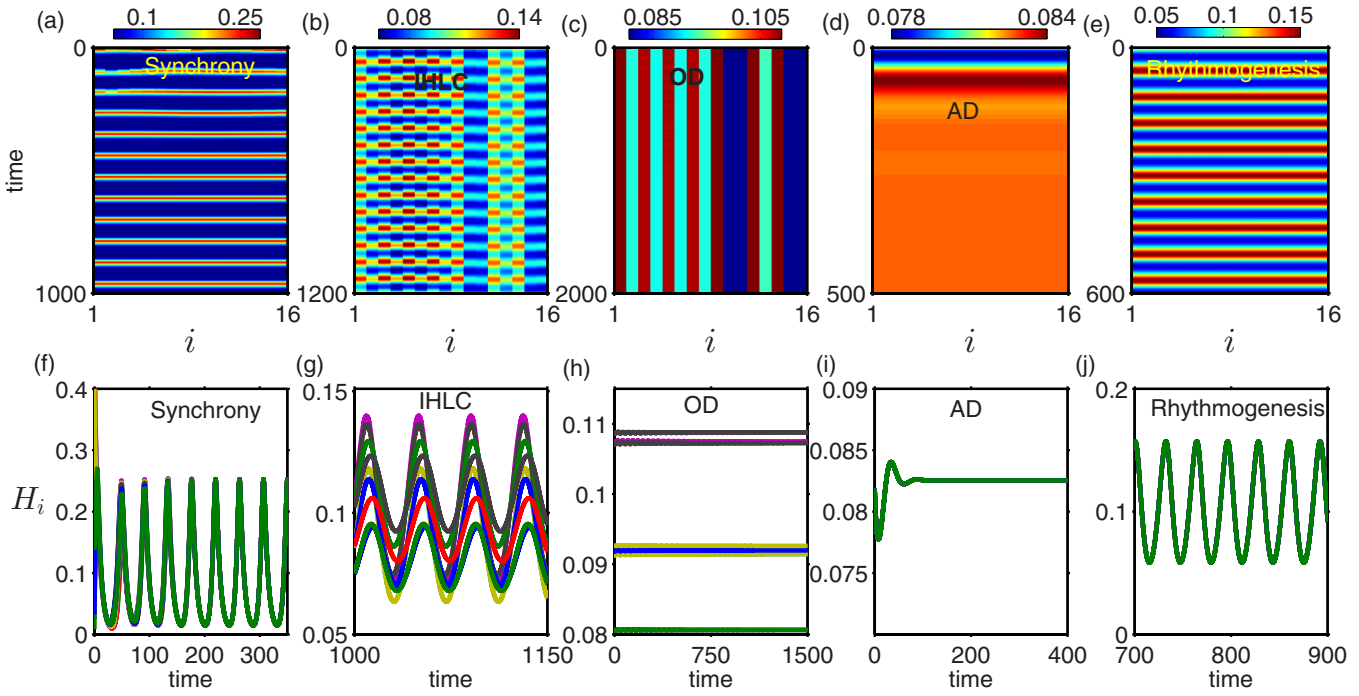

FIG. 9. In a network of 16 patches, spatial dynamics, and time series: (a), (f) for synchronized oscillations for $\epsilon = 0.15$, $d = 0.35$, and $m = 0.2$, (b), (g) synchronized oscillations with inhomogeneous limit cycles for $\epsilon = 0.2369$, $d = 0.35$, and $m = 0.2$, (c), (h) oscillation death for $\epsilon = 0.2058$, $d = 0.35$, and $m = 0.2$, (d), (i) amplitude death for $\epsilon = 0.55$, $d = 0.1$, and $m = 0.2$, and (e), (j) rhythmogenesis for $\epsilon = 0.15$, $d = 0.3$, and $m = 0.3$. Other fixed parameters are $\alpha = 1$, $r = 0.5$, $K = 0.5$, $B = 0.16$, $\beta = 0.5$, $r_1 = 0.8$, $K_1 = 2$, $C = 1$, and $\gamma = 0.6$.

the resource V in the ith patch along with common dynamic environment E are given by

$$\frac{dV_i}{dt} = rV_i\left(1 - \frac{V_i}{K}\right) - \frac{\alpha V_i}{V_i + B}H_i, \tag{2a}$$

$$\frac{dH_i}{dt} = H_i\left(\beta\frac{\alpha V_i}{V_i + B} - m\right) + d(H_{i+1} - 2H_i + H_{i-1}) + \gamma\frac{\epsilon E}{E + C}H_i, \quad i = 1,2,\ldots,N, \tag{2b}$$

$$\frac{dE}{dt} = r_1 E\left(1 - \frac{E}{K_1}\right) - \sum_{i=1}^{N}\frac{\epsilon E}{E + C}H_i\ . \tag{2c}$$

While dispersal takes place, many patches are connected in the network with a common environment and also the area of the dynamic environment is large in a network of 16 patches. Hence we consider a high carrying capacity K_1 of the environment so that it can support many connected patches.

We check the robustness of our results at different levels of the dispersal rate for a network consisting 16 patches and a common dynamic environment. First, for low values of ϵ, Fig. 9(a) shows the synchronized oscillations of 16 patches when dispersal rate $d = 0.35$. A time series of perfectly synchronized HLC of the consumer H is shown in Fig. 9(f).

With an increase in ϵ and choosing appropriate initial conditions, Fig. 9(b) shows inhomogeneous limit cycles for the same dispersal rate $d = 0.35$. Corresponding trajectories are shown in Fig. 9(g). From this, it is clear that consumer species in 16 patches are in-phase synchronized. As like two patches, the network of 16 patches also show AD and OD. Depending on initial conditions, we get either IHLC or oscillation death. Spatiotemporal dynamics and time series of multiclustered OD states are shown in Figs. 9(c) and 9(h), respectively.

For low dispersal rate ($d = 0.1$), AD occurs. The suppression of oscillation in homogeneous steady states is shown in Fig. 9(d) with the time series shown in Fig. 9(i). Occurrence of rhythmogeneis is shown in Figs. 9(e) and 9(j) for $m = 0.3$, $\epsilon = 0.15$, and $d = 0.3$. The environmentally coupled system of a network shows a similar kind of dynamics as shown for two patches. From the collective behavior shown in Fig. 9, it is clear that HLC, IHLC, AD, OD, and rhythmogeneis all are also valid in a network connected by a common dynamic environment.

VI. DISCUSSION

In this section, we discuss the main results of the paper and the importance of the results in ecology.

In most of the previous studies describing the effect of dispersal, the dynamic environment is either excluded or just considered as a static dynamical system. In our study, we specifically reveal that the dynamic environment indeed plays a crucial role in governing the coupled behavior. The detailed bifurcation analysis incorporating both the dynamic environmental coupling and the interpatch dispersal reveal the importance of spatial and environmental heterogeneity in ecosystems.

Our ecological model reveals the mechanism of rhythmogenesis which is interesting also in terms of a dynamical systems point of view. Rhythmogenesis is an emergent process by which the rhythmic behavior of individual oscillators in

a network is restored from an oscillation quenched state without changing the intrinsic parameters associated with the individual nodes. In earlier studies, rhythmogenesis is identified in relaxation oscillators (i.e., in a slow-fast dynamical system) with conjugate coupling [23]. In fact, in relaxation oscillators, when perturbation in the system is sufficiently strong and above some threshold, that leads to generation of oscillations. However, in smooth oscillators, rhythmogenesis is not a trivial process. Once the system is in a death state, special modifications in coupling have to be introduced to revoke that death state and establish rhythmicity [26,35]. For example, Zou *et al.* [26] proposed a technique of inducing rhythmogenesis in Stuart-Landau oscillators with an additional feedback factor in diffusive coupling. Unlike previous studies, here we show that environmental coupling alone can generate oscillation without any feedback factor due to the presence of nonlinearity in the coupling. It is an important finding since in biological system functioning, rhythms and their synchronization play an important role [36,37]. Moreover, the generated oscillation with change in initial conditions determines whether the oscillations are in-phase synchronized or out-of-phase synchronized. Importantly, the dynamic environment acts as a feedback factor and generates the synchronized oscillations in connected patches. In addition to that, with simple diffusive coupling in species dispersal, the coupled system exhibits many interesting dynamics with variability in spatial and environmental parameters. Along with consumer dispersal, the environmental coupling induces the amplitude death and oscillation death. Starting from the generation of oscillations, various synchronization processes in a smooth oscillator and its suppression to different steady states, such as AD, OD, and AD-OD transition, are shown in our coupled ecological system.

As far as ecological systems are concerned, previous studies in a dynamic environment identified two mechanisms of spatial effects, i.e., an increase in species diversity and an increase in community persistence for a longer time [38–40]. Here the formation of homogeneous and inhomogeneous steady states resembles the persistence of a habitat due to characteristics of steady states. Further, our model shows both dispersal induced synchrony and stability simultaneously. However, in ecological systems it is commonly understood that synchrony and stability are two conflicting outcomes of dispersal and both can not be achieved simultaneously [41]. From different steady states and oscillation, the relationship between synchrony and stability induced by dispersal as well as a dynamic environment has been identified. Even though resource density is not directly involved in dispersal, the intrinsic dynamics and the consumer-resource interaction within the patch enables the same qualitative behavior in all the species involved in system.

Earlier, landscape and metapopulation models have been used to predict the species extinction risk and the spatial pattern on ecological processes [19,42,43]. In particular, stochastic models have been used to predict the general features of dynamic habitats [8,9,13]. Although our deterministic model depicts as a metapopulation model, but it explicitly describes various ecological perspectives qualitatively and quantitatively. In particular, dispersal enhances the occurrences of synchronized oscillations and the synchrony-stability relationship, which essentially increases the community persistence from complete extinction. Subsequently, dispersal and climatic perturbations are two strong factors which promote the high level of synchrony. The bifurcation diagram shown here qualitatively determines these consequences through spatial and environmental heterogeneity that identifies the parameter variation in the system due to external perturbations or environmental fluctuations.

Also, due to the presence of noise in ecological systems, oscillating species are prone to extinction easily, so it is important to understand the factors which enhance the synchrony-stability relationship. Although many internal and external factors influence dispersal for successful colonization in the new habitat, but different environmental conditions due to heterogeneity enable the appearance and disappearance of oscillations and transition from homogeneous steady states to inhomogeneous steady states in this system. In general, spatial and environmental heterogeneity clearly distinguish the synchrony-stability relationship induced by both dispersal and a common dynamic environment.

Further, in the context of food web dynamics, food web complexity and species movement pattern contribute largely to enrich the current knowledge [39]. Generally, active as well as passive dispersal take place in natural systems. Specifically, in active dispersal, species are directly involved in movement whereas in passive dispersal, species are being moved by other factors. In this work, we set active dispersal in consumer populations only, but in addition, dispersal also happens in resource populations either directly or indirectly [38,39].

VII. CONCLUSION

In summary, in this paper we have modeled an ecological system connecting local habitats through dispersal in a common environment in which the considered environment is nonlinear and dynamic; at the same time we also consider the interaction between the patches and the environment, which is controlled by ecologically relevant parameters like the conversion efficiency and half saturation constant. We focus on the consumer interaction in three distinct ways, i.e., the interaction within the patch, between the patches, and through the environment. In the presence of dispersal and dynamic environment, these mechanisms are interrelated in the coupled system, which gives rise to several interesting emergent behaviors.

Further, the time scale of dispersal is slow as compared to temporal dynamics within the patch and interconnected habitats are heterogeneous with various network structure. Thus, instead of considering just nearby habitats connectivity, it will be interesting to explore the dispersal effect in a two-dimensional lattice. We believe that much more complex behavior would arise in two dimensions, and our present study will be helpful in proper understanding of those behaviors. Therefore, future study is required to focus on a different kind of dispersal in a higher dimension with different time scales in heterogeneous environments.

ACKNOWLEDGMENTS

We convey our sincere thanks to the anonymous referees for insightful comments. P.S.D. acknowledges financial support

from SERB, Department of Science and Technology (DST), India (Grant No. YSS/2014/000057). T.B. acknowledges the financial support from SERB, Department of Science and Technology (DST), India (Grant No. SB/FTP/PS-005/2013).

[1] I. Hanski, Nature (London) **396**, 41 (1998).
[2] I. Hanski, *Metapopulation Ecology* (Oxford University Press, New York, 1999).
[3] E. E. Goldwyn and A. Hastings, Theor. Popul. Biol. **73**, 395 (2008).
[4] M. D. Holland and A. Hastings, Nature (London) **456**, 792 (2008).
[5] R. Nathan, Proc. Natl. Acad. Sci. USA **105**, 19050 (2008).
[6] E. I. Damschen, L. A. Brudvig, N. M. Haddad, D. J. Levey, J. L. Orrock, and J. J. Tewksbury, Proc. Natl. Acad. Sci. USA **105**, 19078 (2008).
[7] J. K. Cooper, J. Li, and D. J. S. Montagnes, Ecol. Lett. **15**, 856 (2012).
[8] I. Hanski, Oikos **87**, 209 (1999).
[9] D. A. Keith, H. R. Akcakaya, W. Thuiller, G. F. Midgley, R. G. Pearson, S. J. Phillips, H. M. Regan, M. B. Araujo, and T. G. Rebelo, Biol. Lett. **4**, 560 (2008).
[10] T. Banerjee, P. S. Dutta, and A. Gupta, Phys. Rev. E **91**, 052919 (2015).
[11] R. Arumugam, P. S. Dutta, and T. Banerjee, Chaos **25**, 103121 (2015).
[12] J. Vandermeer, BioScience **56**, 967 (2006).
[13] J. E. Keymer, P. A. Marquet, J. X. Velasco-Hernandez, and S. A. Levin, Am. Nat. **156**, 478 (2000).
[14] G. Katriel, Phys. D (Amsterdam, Neth.) **237**, 2933 (2008).
[15] V. Resmi, G. Ambika, and R. E. Amritkar, Phys. Rev. E **81**, 046216 (2010).
[16] V. Resmi, G. Ambika, and R. E. Amritkar, Phys. Rev. E **84**, 046212 (2011).
[17] V. Resmi, G. Ambika, R. E. Amritkar, and G. Rangarajan, Phys. Rev. E **85**, 046211 (2012).
[18] D. Ghosh and T. Banerjee, Phys. Rev. E **90**, 062908 (2014).
[19] W. Gu, R. Heikkilä, and I. Hanski, Landscape Ecol. **17**, 699 (2002).
[20] T. Mueller, R. B. O'Hara, S. J. Converse, R. P. Urbanek, and W. F. Fagan, Science **341**, 999 (2013).
[21] S. H. Strogatz, *Nonlinear Dynamics and Chaos*, 1st ed. (Addison-Wesley Publishing Company, Reading, MA, 1994).
[22] W. W. Murdoch, C. J. Briggs, and R. M. Nisbet, *Consumer–Resource Dynamics* (Princeton University Press, New Jersey, 2003).
[23] M. Dasgupta, M. Rivera, and P. Parmananda, Chaos **20**, 023126 (2010).
[24] A. Chakraborty, A. Ray, S. Basak, and A. R. Chowdhury, Phys. Lett. A **379**, 1418 (2015).
[25] L. Glass, Nature (London) **410**, 277 (2001).
[26] W. Zou, D. V. Senthilkumar, R. Nagao, I. Z. Kiss, Y. Tang, A. Koseska, J. Duan, and J. Kurths, Nat. Commun. **6**, 7709 (2015).
[27] Y. Loewenstein, Y. Yarom, and H. Sompolinsky, Proc. Natl. Acad. Sci. USA **98**, 8095 (2001).
[28] R. M. Harris-Warrick, Prog. Brain Res. **187**, 213 (2010).
[29] A. Koseska, E. Volkov, and J. Kurths, Phys. Rep. **531**, 173 (2013).
[30] A. Koseska, E. Volkov, and J. Kurths, Phys. Rev. Lett. **111**, 024103 (2013).
[31] P. S. Dutta and T. Banerjee, Phys. Rev. E **92**, 042919 (2015).
[32] M. L. Rosenzweig and R. H. MacArthur, Am. Nat. **97**, 209 (1963).
[33] C. S. Holling, Can. Entomol. **91**, 385 (1959).
[34] B. Ermentrout, *Simulating, Analyzing, and Animating Dynamical Systems: A Guide to Xppaut for Researchers and Students (Software, Environments, Tools)* (SIAM Press, Philadelphia, 2002).
[35] A. Majdandzic, B. Podobnik, S. V. Buldyrev, D. Y. Kenett, S. Havlin, and H. E. Stanley, Nat. Phys. **10**, 34 (2013); W. Zou, D. V. Senthilkumar, M. Zhan, and J. Kurths, Phys. Rev. Lett. **111**, 014101 (2013); D. Ghosh, T. Banerjee, and J. Kurths, Phys. Rev. E **92**, 052908 (2015).
[36] L. Glass and M. C. Mackey, *From Clocks to Chaos: The Rhythms of Life* (Princeton University Press, Princeton, 1988).
[37] A. Goldbeter, *Biochemical Oscillations and Cellular Rhythms: The Molecular Bases of Periodic and Chaotic Behaviour* (Cambridge University Press, Cambridge, 1996).
[38] A. Liebhold, W. D. Koenig, and O. N. Bjørnstad, Ann. Rev. Ecol., Evol., Syst. **35**, 467 (2004).
[39] P. Amarasekare, Ann. Rev. Ecol., Evol., Syst. **39**, 479 (2008).
[40] K. Johst, R. Brandl, and S. Eber, Oikos **98**, 263 (2002).
[41] C. J. Briggs and M. F. Hoopes, Theor. Popul. Biol. **65**, 299 (2004).
[42] H. R. Akcakaya, V. C. Radeloff, D. J. Mladenoff, and H. S. He, Conserv. Biol. **18**, 526 (2004).
[43] M. C. Wimberly, Landscape Ecol. **21**, 35 (2006).